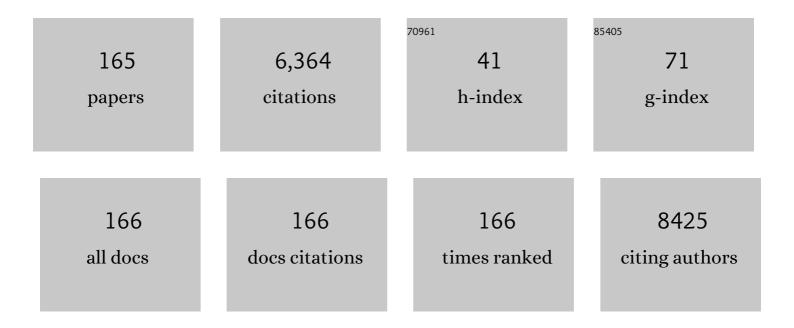
List of Publications by Year in descending order

Source: https://exaly.com/author-pdf/4447960/publications.pdf Version: 2024-02-01



ΥΠΥΝ-DI ΖΗΛΟ

#	Article	IF	CITATIONS
1	Recent advances in electrochemical sensing for hydrogen peroxide: a review. Analyst, The, 2012, 137, 49-58.	1.7	826
2	The interface behavior of hemoglobin at carbon nanotube and the detection for HO. Talanta, 2005, 65, 489-494.	2.9	174
3	Direct electrochemistry of horseradish peroxidase at carbon nanotube powder microelectrode. Sensors and Actuators B: Chemical, 2002, 87, 168-172.	4.0	167
4	A pH/Ultrasound dual-response biomimetic nanoplatform for nitric oxide gas-sonodynamic combined therapy and repeated ultrasound for relieving hypoxia. Biomaterials, 2020, 230, 119636.	5.7	164
5	Anodic oxidation of hydrazine at carbon nanotube powder microelectrode and its detection. Talanta, 2002, 58, 529-534.	2.9	160
6	ROS-augmented and tumor-microenvironment responsive biodegradable nanoplatform for enhancing chemo-sonodynamic therapy. Biomaterials, 2020, 234, 119761.	5.7	144
7	Electrocatalytic oxidation of phytohormone salicylic acid at copper nanoparticles-modified gold electrode and its detection in oilseed rape infected with fungal pathogen Sclerotinia sclerotiorum. Talanta, 2010, 80, 1277-1281.	2.9	132
8	Direct Electron Transfer of Glucose Oxidase Molecules Adsorbed onto Carbon Nanotube Powder Microelectrode Analytical Sciences, 2002, 18, 939-941.	0.8	123
9	Designer Exosomes for Active Targeted Chemoâ€Photothermal Synergistic Tumor Therapy. Advanced Functional Materials, 2018, 28, 1707360.	7.8	120
10	Red blood cell membrane-enveloped O ₂ self-supplementing biomimetic nanoparticles for tumor imaging-guided enhanced sonodynamic therapy. Theranostics, 2020, 10, 867-879.	4.6	117
11	Electrocatalytic oxidation of cysteine at carbon nanotube powder microelectrode and its detection. Sensors and Actuators B: Chemical, 2003, 92, 279-285.	4.0	106
12	Nitrogen-doped graphene quantum dot for direct fluorescence detection of Al3+ in aqueous media and living cells. Biosensors and Bioelectronics, 2018, 100, 41-48.	5.3	104
13	Temperature-dependent photoluminescence of water-soluble quantum dots for a bioprobe. Analytica Chimica Acta, 2006, 559, 120-123.	2.6	84
14	Distance-Dependent Metal-Enhanced Quantum Dots Fluorescence Analysis in Solution by Capillary Electrophoresis and Its Application to DNA Detection. Analytical Chemistry, 2011, 83, 4103-4109.	3.2	79
15	High quantum yield Ag ₂ S quantum dot@polypeptide-engineered hybrid nanogels for targeted second near-infrared fluorescence/photoacoustic imaging and photothermal therapy. Chemical Communications, 2018, 54, 527-530.	2.2	77
16	Purification of denatured bovine serum albumin coated CdTe quantum dots for sensitive detection of silver(I) ions. Analytical and Bioanalytical Chemistry, 2007, 388, 969-974.	1.9	75
17	Some characteristics and functional properties of rapeseed protein prepared by ultrasonication, ultrafiltration and isoelectric precipitation. Journal of the Science of Food and Agriculture, 2011, 91, 1488-1498.	1.7	72
18	Folic acid-conjugated silica-coated gold nanorods and quantum dots for dual-modality CT and fluorescence imaging and photothermal therapy. Journal of Materials Chemistry B, 2014, 2, 1945.	2.9	71

#	Article	IF	CITATIONS
19	Increased electrocatalyzed performance through hairpin oligonucleotide aptamer-functionalized gold nanorods labels and graphene-streptavidin nanomatrix: Highly selective and sensitive electrochemical biosensor of carcinoembryonic antigen. Biosensors and Bioelectronics, 2016, 83, 142-148.	5.3	67
20	Simultaneous detection of dual single-base mutations by capillary electrophoresis using quantum dot-molecular beacon probe. Biosensors and Bioelectronics, 2011, 26, 2317-2322.	5.3	66
21	High-sensitivity quantum dot-based fluorescence resonance energy transfer bioanalysis by capillary electrophoresis. Biosensors and Bioelectronics, 2010, 25, 1283-1289.	5.3	65
22	A new strategy for the detection of adenosine triphosphate by aptamer/quantum dot biosensor based on chemiluminescence resonance energy transfer. Analyst, The, 2012, 137, 4262.	1.7	62
23	Capillary electrophoresis-chemiluminescence detection for carcino-embryonic antigen based on aptamer/graphene oxide structure. Biosensors and Bioelectronics, 2015, 64, 493-498.	5.3	62
24	Intelligent gold nanostars for <i>in vivo</i> CT imaging and catalase-enhanced synergistic photodynamic & photothermal tumor therapy. Theranostics, 2019, 9, 5424-5442.	4.6	61
25	One-step fabrication of poly(o-aminophenol)/multi-walled carbon nanotubes composite film modified electrode and its application for levofloxacin determination in pharmaceuticals. Sensors and Actuators B: Chemical, 2012, 174, 202-209.	4.0	57
26	Influence of quantum dot's quantum yield to chemiluminescent resonance energy transfer. Analytica Chimica Acta, 2008, 610, 68-73.	2.6	56
27	Carcino-embryonic antigen detection based on fluorescence resonance energy transfer between quantum dots and graphene oxide. Biosensors and Bioelectronics, 2014, 59, 397-403.	5.3	55
28	Multifunctional quantum dot–polypeptide hybrid nanogel for targeted imaging and drug delivery. Nanoscale, 2014, 6, 11282-11292.	2.8	55
29	Electrocatalytic activity of salicylic acid on the platinum nanoparticles modified electrode by electrochemical deposition. Colloids and Surfaces B: Biointerfaces, 2010, 76, 370-374.	2.5	53
30	Discovery of 5-Cyano-6-phenylpyrimidin Derivatives Containing an Acylurea Moiety as Orally Bioavailable Reversal Agents against P-Glycoprotein-Mediated Mutidrug Resistance. Journal of Medicinal Chemistry, 2018, 61, 5988-6001.	2.9	53
31	Characterization of the coupling of quantum dots and immunoglobulin antibodies. Analytical and Bioanalytical Chemistry, 2006, 386, 1665-1671.	1.9	52
32	Novel pyrimidine-based amphiphilic molecules: synthesis, spectroscopic properties and applications in two-photon fluorescence microscopic imaging. Journal of Materials Chemistry, 2007, 17, 2921.	6.7	52
33	Targeted quantum dots fluorescence probes functionalized with aptamer and peptide for transferrin receptor on tumor cells. Nanotechnology, 2012, 23, 485104.	1.3	52
34	In Vivo Computed Tomography/Photoacoustic Imaging and NIR-Triggered Chemo–Photothermal Combined Therapy Based on a Gold Nanostar-, Mesoporous Silica-, and Thermosensitive Liposome-Composited Nanoprobe. ACS Applied Materials & Interfaces, 2017, 9, 41748-41759.	4.0	52
35	Highâ€Security Nanocluster for Switching Photodynamic Combining Photothermal and Acidâ€Induced Drug Compliance Therapy Guided by Multimodal Activeâ€Targeting Imaging. Advanced Functional Materials, 2018, 28, 1803118.	7.8	48
36	In vivo cancer targeting and fluorescence-CT dual-mode imaging with nanoprobes based on silver sulfide quantum dots and iodinated oil. Nanoscale, 2015, 7, 19484-19492.	2.8	47

ΥUAN-DI ΖΗΑΟ

#	Article	IF	CITATIONS
37	Hydrogen peroxide biosensor based on direct electron transfer of horseradish peroxidase with vapor deposited quantum dots. Sensors and Actuators B: Chemical, 2009, 138, 278-282.	4.0	46
38	<i>In vivo</i> Imaging-Guided Nanoplatform for Tumor Targeting Delivery and Combined Chemo-, Gene- and Photothermal Therapy. Theranostics, 2018, 8, 5662-5675.	4.6	46
39	Facile Synthesis of Gold Nanospheres Modified by Positively Charged Mesoporous Silica, Loaded with Near-Infrared Fluorescent Dye, for in Vivo X-ray Computed Tomography and Fluorescence Dual Mode Imaging. ACS Applied Materials & Interfaces, 2015, 7, 17287-17297.	4.0	45
40	Ultrafast synthesis of gold nanosphere cluster coated by graphene quantum dot for active targeting PA/CT imaging and near-infrared laser/pH-triggered chemo-photothermal synergistic tumor therapy. Chemical Engineering Journal, 2019, 369, 87-99.	6.6	45
41	A highly sensitive nitric oxide biosensor based on hemoglobin–chitosan/graphene–hexadecyltrimethylammonium bromide nanomatrix. Sensors and Actuators B: Chemical, 2012, 166-167, 444-450.	4.0	44
42	Targeting N-doped graphene quantum dot with high photothermal conversion efficiency for dual-mode imaging and therapy <i>in vitro</i> . Nanotechnology, 2018, 29, 355101.	1.3	44
43	An injectable hybrid hydrogel based on a genetically engineered polypeptide for second near-infrared fluorescence/photoacoustic imaging-monitored sustained chemo-photothermal therapy. Nanoscale, 2019, 11, 16080-16091.	2.8	43
44	Applications of gold nanorods in biomedical imaging and related fields. Science Bulletin, 2013, 58, 2530-2536.	1.7	41
45	A novel oriented immobilized lipase on magnetic nanoparticles in reverse micelles system and its application in the enrichment of polyunsaturated fatty acids. Bioresource Technology, 2013, 132, 99-102.	4.8	41
46	The oxidation and reduction behavior of nitrite at carbon nanotube powder microelectrodes. Microchemical Journal, 2003, 75, 189-198.	2.3	40
47	Antitumor immunity triggered by photothermal therapy and photodynamic therapy of a 2D MoS ₂ nanosheet-incorporated injectable polypeptide-engineered hydrogel combinated with chemotherapy for 4T1 breast tumor therapy. Nanotechnology, 2020, 31, 205102.	1.3	39
48	Tumor Microenvironment-Activated Theranostics Nanozymes for Fluorescence Imaging and Enhanced Chemo-Chemodynamic Therapy of Tumors. ACS Applied Materials & Interfaces, 2021, 13, 55780-55789.	4.0	39
49	Tracking the Downâ€Regulation of Folate Receptorâ€Î± in Cancer Cells through Target Specific Delivery of Quantum Dots Coupled with Antisense Oligonucleotide and Targeted Peptide. Small, 2013, 9, 4183-4193.	5.2	38
50	A highly efficient capillary electrophoresis-based method for size determination of water-soluble CdSe/ZnS core–shell quantum dots. Analytica Chimica Acta, 2009, 647, 219-225.	2.6	37
51	Immobilized protease on the magnetic nanoparticles used for the hydrolysis of rapeseed meals. Journal of Magnetism and Magnetic Materials, 2010, 322, 2031-2037.	1.0	36
52	Graphene nanopores toward DNA sequencing: a review of experimental aspects. Science China Chemistry, 2017, 60, 721-729.	4.2	36
53	Highâ€Security Multifunctional Nanoâ€Bismuthâ€Sphereâ€Cluster Prepared from Oral Gastric Drug for CT/PA Dualâ€Mode Imaging and Chemoâ€Photothermal Combined Therapy In Vivo. Advanced Functional Materials, 2019, 29, 1900017.	7.8	36
54	A flow cytometric assay technology based on quantum dots-encoded beads. Analytica Chimica Acta, 2006, 580, 18-23.	2.6	35

#	Article	IF	CITATIONS
55	Multi-color encoding of polystyrene microbeads with CdSe/ZnS quantum dots and its application in immunoassay. Journal of Colloid and Interface Science, 2007, 316, 622-627.	5.0	35
56	A novel amperometric adenosine triphosphate biosensor by immobilizing graphene/dual-labeled aptamers complex onto poly(o-phenylenediamine) modified electrode. Sensors and Actuators B: Chemical, 2014, 191, 695-702.	4.0	34
57	Synthesis and biological evaluation of new steroidal pyridines as potential anti-prostate cancer agents. European Journal of Medicinal Chemistry, 2018, 145, 11-22.	2.6	34
58	A NanoFlareâ€Based Strategy for In Situ Tumor Margin Demarcation and Neoadjuvant Gene/Photothermal Therapy. Small, 2018, 14, e1802745.	5.2	34
59	Injectable polypeptide-engineered hydrogel depot for amplifying the anti-tumor immune effect induced by chemo-photothermal therapy. Journal of Materials Chemistry B, 2020, 8, 8623-8633.	2.9	34
60	<i>In situ</i> aqueous synthesis of genetically engineered polypeptide-capped Ag ₂ S quantum dots for second near-infrared fluorescence/photoacoustic imaging and photothermal therapy. Journal of Materials Chemistry B, 2019, 7, 2484-2492.	2.9	33
61	In vivo monitoring of oxidative burst on aloe under salinity stress using hemoglobin and single-walled carbon nanotubes modified carbon fiber ultramicroelectrode. Biosensors and Bioelectronics, 2013, 50, 318-324.	5.3	31
62	LPE-1, an orally active pyrimidine derivative, inhibits growth and mobility of human esophageal cancers by targeting LSD1. Pharmacological Research, 2017, 122, 66-77.	3.1	31
63	Photoluminescence enhancement by coupling of ovalbumin and CdTe quantum dots and its application as protein probe. Colloids and Surfaces A: Physicochemical and Engineering Aspects, 2007, 305, 48-53.	2.3	30
64	Interaction of CdTe quantum dots with DNA. Electrochemistry Communications, 2008, 10, 1337-1339.	2.3	30
65	<i>In vivo</i> tumor active cancer targeting and CT-fluorescence dual-modal imaging with nanoprobe based on gold nanorods and InP/ZnS quantum dots. Journal of Materials Chemistry B, 2018, 6, 2574-2583.	2.9	30
66	Graphene oxide-assisted Au nanoparticle strip biosensor based on GR-5 DNAzyme for rapid lead ion detection. Colloids and Surfaces B: Biointerfaces, 2018, 169, 305-312.	2.5	30
67	Reverse microemulsion-mediated synthesis of Bi2S3–QD@SiO2–PEG for dual modal CT–fluorescence imaging in vitro and in vivo. Chemical Communications, 2013, 49, 11800.	2.2	29
68	HIV-related DNA detection through switching on hybridized quenched fluorescent DNA-Ag nanoclusters. Nanoscale, 2018, 10, 5532-5538.	2.8	29
69	Graphene oxide coating core–shell silver sulfide@mesoporous silica for active targeted dual-mode imaging and chemo-photothermal synergistic therapy against tumors. Journal of Materials Chemistry B, 2018, 6, 4808-4820.	2.9	29
70	Directed self-assembly of polypeptide-engineered physical microgels for building porous cell-laden hydrogels. Chemical Communications, 2014, 50, 9405-9408.	2.2	28
71	Polypeptide-Engineered Hydrogel Coated Gold Nanorods for Targeted Drug Delivery and Chemo-photothermal Therapy. ACS Biomaterials Science and Engineering, 2017, 3, 2391-2398.	2.6	28
72	<i>In vitro</i> and <i>in vivo</i> CT imaging using bismuth sulfide modified with a highly biocompatible Pluronic F127. Nanotechnology, 2014, 25, 295103.	1.3	27

#	Article	IF	CITATIONS
73	Detection of alkaline phosphatase activity with a functionalized nanopipette. Electrochemistry Communications, 2019, 99, 71-74.	2.3	27
74	A smartphone-based rapid quantitative detection platform for lateral flow strip of human chorionic gonadotropin with optimized image algorithm. Microchemical Journal, 2020, 157, 105038.	2.3	27
75	Study on molecular interactions between proteins on live cell membranes using quantum dot-based fluorescence resonance energy transfer. Analytical and Bioanalytical Chemistry, 2008, 391, 2819-2824.	1.9	25
76	One-Step in Situ Synthesis of Polypeptide–Gold Nanoparticles Hybrid Nanogels and Their Application in Targeted Photoacoustic Imaging. ACS Sustainable Chemistry and Engineering, 2017, 5, 9841-9847.	3.2	25
77	A near-infrared light-controlled smart nanocarrier with reversible polypeptide-engineered valve for targeted fluorescence-photoacoustic bimodal imaging-guided chemo-photothermal therapy. Theranostics, 2019, 9, 7666-7679.	4.6	25
78	Composite silica coated gold nanosphere and quantum dots nanoparticles for X-ray CT and fluorescence bimodal imaging. Dalton Transactions, 2015, 44, 11314-11320.	1.6	24
79	Optimization of the methods for introduction of amine groups onto the silica nanoparticle surface. Journal of Biomedical Materials Research - Part A, 2007, 80A, 752-757.	2.1	23
80	Bioconjugate recognition molecules to quantum dots as tumor probes. Journal of Biomedical Materials Research - Part A, 2007, 83A, 1209-1216.	2.1	23
81	Solubilization and bioconjugation of QDs and their application in cell imaging. Journal of Biomedical Materials Research - Part A, 2008, 86A, 833-841.	2.1	23
82	In Vivo Electrochemical Biosensors for Reactive Oxygen Species Detection: A Mini-Review. Analytical Letters, 2012, 45, 156-167.	1.0	23
83	Synthesis and characterization of Bi2S3 composite nanoparticles with high X-ray absorption. Materials Research Bulletin, 2013, 48, 3800-3804.	2.7	23
84	Hybrid nanoprobes of bismuth sulfide nanoparticles and CdSe/ZnS quantum dots for mouse computed tomography/fluorescence dual mode imaging. Journal of Nanobiotechnology, 2015, 13, 76.	4.2	23
85	Quantum dot-modified aptamer probe for chemiluminescence detection of carcino-embryonic antigen using capillary electrophoresis. Sensors and Actuators B: Chemical, 2015, 210, 158-164.	4.0	23
86	Bismuth particles imbedded degradable nanohydrogel prepared by one-step method for tumor dual-mode imaging and chemo-photothermal combined therapy. Chemical Engineering Journal, 2019, 375, 122000.	6.6	23
87	A multifunctional targeting probe with dual-mode imaging and photothermal therapy used in vivo. Journal of Nanobiotechnology, 2018, 16, 42.	4.2	22
88	Visual simultaneous detection of single nucleotide polymorphism of tumor susceptibility gene and marker alpha-fetoprotein based on double-labeled colloidal gold probe with lateral ï¬,ow strip biosensor. Sensors and Actuators B: Chemical, 2019, 298, 126819.	4.0	22
89	Hybridization induced fluorescence enhanced DNA-Ag nanocluster/aptamer probe for detection of prostate-specific antigen. Colloids and Surfaces B: Biointerfaces, 2019, 175, 358-364.	2.5	22
90	Polypeptide-engineered physical hydrogels designed from the coiled-coil region of cartilage oligomeric matrix protein for three-dimensional cell culture. Journal of Materials Chemistry B, 2014, 2, 3123-3132.	2.9	21

#	Article	IF	CITATIONS
91	The interface behavior and biocatalytic activity of superoxide dismutase at carbon nanotube. Biosensors and Bioelectronics, 2006, 21, 1350-1354.	5.3	20
92	High transfection efficiency of quantum dot-antisense oligonucleotide nanoparticles in cancer cells through dual-receptor synergistic targeting. Nanotechnology, 2014, 25, 255102.	1.3	20
93	A near-infrared light-controlled system for reversible presentation of bioactive ligands using polypeptide-engineered functionalized gold nanorods. Chemical Communications, 2015, 51, 2569-2572.	2.2	20
94	One-pot two-step synthesis of core–shell mesoporous silica-coated gold nanoparticles. Dalton Transactions, 2015, 44, 7752-7756.	1.6	20
95	Visual detection of trace lead ion based on aptamer and silver staining nano-metal composite. Colloids and Surfaces B: Biointerfaces, 2018, 162, 415-419.	2.5	20
96	Visual detection of Pb2+ using strip biosensor based on PS2M aptamer and sensitivity enhancement probe. Sensors and Actuators B: Chemical, 2018, 261, 307-315.	4.0	20
97	Hollow gold nanoshells-incorporated injectable genetically engineered hydrogel for sustained chemo-photothermal therapy of tumor. Journal of Nanobiotechnology, 2019, 17, 99.	4.2	20
98	Development of dual strip biosensors based on hybridization chain reaction and microplate strategies for signal amplification of HBV-DNA detection. Sensors and Actuators B: Chemical, 2020, 310, 127829.	4.0	20
99	A pH/ultrasonic dual-response step-targeting enterosoluble granule for combined sonodynamic-chemotherapy guided <i>via</i> gastrointestinal tract imaging in orthotopic colorectal cancer. Nanoscale, 2021, 13, 4278-4294.	2.8	20
100	Optimisation of preparation conditions and properties of phytosterol liposome-encapsulating nattokinase. Natural Product Research, 2012, 26, 548-556.	1.0	19
101	Detection of adenosine triphosphate in HeLa cell using capillary electrophoresis-laser induced fluorescence detection based on aptamer and graphene oxide. Colloids and Surfaces B: Biointerfaces, 2016, 140, 233-238.	2.5	19
102	pH-modulated ion-current rectification in a cysteine-functionalized glass nanopipette. Electrochemistry Communications, 2018, 97, 6-10.	2.3	19
103	Highly efficient MnO2/reduced graphene oxide hydrogel motors for organic pollutants removal. Journal of Materials Science, 2020, 55, 1984-1995.	1.7	19
104	Simple and accurate visual detection of single nucleotide polymorphism based on colloidal gold nucleic acid strip biosensor and primer-specific PCR. Analytica Chimica Acta, 2020, 1093, 106-114.	2.6	19
105	One-for-All Nanoplatform for Synergistic Mild Cascade-Potentiated Ultrasound Therapy Induced with Targeting Imaging-Guided Photothermal Therapy. ACS Applied Materials & Interfaces, 2020, 12, 40052-40066.	4.0	19
106	A metal ion-drug-induced self-assembly nanosystems for augmented chemodynamic and chemotherapy synergetic anticancer therapy. Carbon, 2022, 188, 104-113.	5.4	19
107	Advancing interfacial properties of carbon cloth via anodic-induced self-assembly of MOFs film integrated with α-MnO2: A sustainable electrocatalyst sensing acetylcholine. Journal of Hazardous Materials, 2022, 426, 128133.	6.5	19
108	Ascorbic acid biosensor based on laccase immobilized on an electrode modified with a self-assembled monolayer and coated with functionalized quantum dots. Mikrochimica Acta, 2009, 165, 387-392.	2.5	18

#	Article	IF	CITATIONS
109	Ion-current-rectification-based customizable pH response in glass nanopipettes via silanization. Electrochemistry Communications, 2018, 93, 95-99.	2.3	18
110	Two-photon-excited fluorescence and two-photon spectrofluoroelectrochemistry of riboflavin. Electrochemistry Communications, 2006, 8, 595-599.	2.3	17
111	Special method to prepare quantum dot probes with reduced cytotoxicity and increased optical property. Journal of Biomedical Optics, 2010, 15, 015001.	1.4	17
112	Preparation, Modification, and Application of Hollow Gold Nanospheres. Journal of Nanomaterials, 2015, 2015, 1-7.	1.5	17
113	A field-compatible technique using an electrochemical sensing microbundle for real-time and simultaneous in vivo measurement of hydrogen peroxide, nitric oxide, and pH under drought stress. Sensors and Actuators B: Chemical, 2015, 220, 743-748.	4.0	17
114	A Feasible and Quantitative Encoding Method for Microbeads with Multicolor Quantum Dots. Journal of Fluorescence, 2007, 17, 133-138.	1.3	16
115	In vivo monitoring of oxidative burst induced by ultraviolet A and C stress for oilseed rape by microbiosensor. Sensors and Actuators B: Chemical, 2009, 141, 599-603.	4.0	16
116	Characterization of CdTe/CdSe quantum dots-transferrin fluorescent probes for cellular labeling. Analytica Chimica Acta, 2012, 741, 86-92.	2.6	16
117	Recent advances in ionic current rectification based nanopore sensing: a mini-review. Sensors and Actuators Reports, 2021, 3, 100042.	2.3	16
118	Detection of multiple mycotoxins based on catalytic hairpin assembly coupled with pregnancy test strip. Sensors and Actuators B: Chemical, 2022, 350, 130911.	4.0	16
119	Fluorescence resonance energy transfer between FITC and water-soluble CdSe/ZnS quantum dots. Colloids and Surfaces A: Physicochemical and Engineering Aspects, 2007, 302, 168-173.	2.3	15
120	Microsensor in vivo monitoring of oxidative burst in oilseed rape (Brassica napus L.) leaves infected by Sclerotinia sclerotiorum. Analytica Chimica Acta, 2009, 632, 21-25.	2.6	15
121	Ion Current Rectification Behavior of Conical Nanopores Filled with Spatially Distributed Fixed Charges. Journal of Physical Chemistry C, 2019, 123, 26299-26308.	1.5	15
122	A self-assembled nanoplatform based on Ag2S quantum dots and tellurium nanorods for combined chemo-photothermal therapy guided by H2O2-activated near-infrared-II fluorescence imaging. Acta Biomaterialia, 2022, 140, 547-560.	4.1	15
123	Folic acid modified Pluronic F127 coating Ag ₂ S quantum dot for photoacoustic imaging of tumor cell-targeting. Nanotechnology, 2018, 29, 055101.	1.3	14
124	Hithertoâ€Unexplored Photodynamic Therapy of Ag ₂ S and Enhanced Regulation Based on Polydopamine In Vitro and Vivo. Chemistry - A European Journal, 2019, 25, 7553-7560.	1.7	13
125	Quantitative analysis of various targets based on aptamer and functionalized Fe3O4@graphene oxide in dairy products using pregnancy test strip and smartphone. Food Chemistry, 2021, 352, 129330.	4.2	13
126	Lateral flow biosensor for universal detection of various targets based on hybridization chain reaction amplification strategy with pregnancy test strip. Sensors and Actuators B: Chemical, 2021, 337, 129778.	4.0	12

#	Article	IF	CITATIONS
127	In vivo measurements of changes in pH triggered by oxalic acid in leaf tissue of transgenic oilseed rape. Phytochemical Analysis, 2007, 18, 341-346.	1.2	11
128	Chemiluminescence detection of lead (II) using â€~8–17' DNAzyme and hemin/G-quadruplex with high sensitivity and selectivity. Sensors and Actuators B: Chemical, 2014, 201, 496-502.	4.0	11
129	Folic acid-targeted magnetic Tb-doped CeF ₃ fluorescent nanoparticles as bimodal probes for cellular fluorescence and magnetic resonance imaging. Dalton Transactions, 2015, 44, 16304-16312.	1.6	11
130	Ion Current Rectification in High-Salt Environment from Mesoporous TiO ₂ Microplug <i>in Situ</i> Grown at the Tip of a Micropipette Induced by Space-Confined Evaporation. Analytical Chemistry, 2019, 91, 15377-15381.	3.2	11
131	Vibrational spectroscopic encoding of polystyrene resin bead: a combined FT-IR and computational study. Journal of Molecular Structure, 2005, 738, 155-159.	1.8	9
132	Biosensor for Hydrogen Peroxide Based on Chitosan and Nanoparticle Complex Film–Modified Glassy-Carbon Electrodes. Analytical Letters, 2009, 42, 2496-2508.	1.0	9
133	Electrocatalysis of emodin at multi-wall nanotubes. Bioelectrochemistry, 2008, 72, 155-160.	2.4	8
134	<i>In vivo</i> monitor oxidative burst induced by Cd ²⁺ stress for the oilseed rape (Brassica napus L.) based on electrochemical microbiosensor. Phytochemical Analysis, 2010, 21, 192-196.	1.2	8
135	Seed-Mediated Synthesis of Polypeptide-Engineered Stabilized Fluorescence-Enhanced Core/Shell Ag ₂ S Quantum Dots and Their Application in pH Sensing and Bacterial Imaging in Extreme Acidity. ACS Sustainable Chemistry and Engineering, 2019, 7, 13098-13104.	3.2	8
136	Ultrasensitive and regenerable nanopore sensing based on target induced aptamer dissociation. Biosensors and Bioelectronics, 2020, 152, 112011.	5.3	8
137	An in situ synthesis of silver nanoparticle-loaded genetically engineered polypeptide nanogels for antibacterial and wound healing applications. Dalton Transactions, 2020, 49, 12049-12055.	1.6	8
138	In situ synthesis of multifunctional tellurium nanorods stabilized by polypeptide-engineered for photothermal-sonodynamic combination therapy of tumors. Chemical Engineering Journal, 2021, 417, 127989.	6.6	8
139	Light-controlled microbots gathering as a sterilization platform for highly efficient capturing, concentrating and killing targeted bacteria. Chemical Engineering Journal, 2022, 435, 135067.	6.6	8
140	lon current rectification in combination with ion current saturation. Analytica Chimica Acta, 2020, 1117, 35-40.	2.6	7
141	Light-controlled spiky micromotors for efficient capture and transport of targets. Sensors and Actuators B: Chemical, 2022, 358, 131523.	4.0	7
142	Extension of duplex specific nuclease sensing application with RNA aptamer. Talanta, 2022, 242, 123314.	2.9	7
143	Real-time observation of the effect of iron on receptor-mediated endocytosis of transferrin conjugated with quantum dots. Journal of Biomedical Optics, 2010, 15, 1.	1.4	6
144	Facile synthesis of carbon nanotube-inorganic hybrid materials with improved photoactivity. Dalton Transactions, 2013, 42, 15280.	1.6	6

#	Article	IF	CITATIONS
145	Multifunctional nanocarrier with self-catalytic production of nitric oxide for photothermal and gas-combined therapy of tumor. Journal of Colloid and Interface Science, 2022, 621, 77-90.	5.0	6
146	Directional and on-demand ion transport regulated by pH and voltage in submicrochannel heteromembrane based on conducting polymer. Chemical Engineering Journal, 2022, 444, 136548.	6.6	6
147	A feasible method of improving the quantum yield of CdTe/CdS quantum dots by the first heating–cooling cycle and their application in cancer cell recognition. Journal of Nanoparticle Research, 2010, 12, 1687-1695.	0.8	5
148	Controllable ion transport induced by pH gradient in a thermally crosslinked submicrochannel heterogeneous membrane. Analyst, The, 2021, 146, 6815-6821.	1.7	5
149	Nanoplaform based on ultra-small Au regulating phototoxicity and fluorescence off–on function of Ag2S for multi-modal diagnosis and treatment of tumor. Chemical Engineering Journal, 2022, 431, 133212.	6.6	5
150	Controlled release of metal phenolic network protected phage for treating bacterial infection. Nanotechnology, 2022, 33, 165102.	1.3	5
151	Evaporative deposition of lipophilic quantum dots for an enzyme modified electrode. Mikrochimica Acta, 2009, 166, 133-138.	2.5	4
152	Labeling of liver cells with CdSe/ZnS quantum dot-based fluorescence probe below freezing point. Spectrochimica Acta - Part A: Molecular and Biomolecular Spectroscopy, 2021, 263, 120203.	2.0	4
153	SELF-ASSEMBLED QUANTUM DOTS ON AU AND THE INTERFACE FLUORESCENCE. Journal of Innovative Optical Health Sciences, 2010, 03, 315-320.	0.5	3
154	Facile fabrication of TiO2-based composites with tunable properties and improved performance through a general and controllable method. RSC Advances, 2013, 3, 4880.	1.7	3
155	Composite nanoparticle of Au and quantum dots for X-ray computed tomography and fluorescence dual-mode imaging in vivo. Journal of Nanoparticle Research, 2015, 17, 1.	0.8	3
156	Fabrication of genetically engineered polypeptide@quantum dots hybrid nanogels for targeted imaging. Journal of Nanoparticle Research, 2017, 19, 1.	0.8	3
157	A simple fluorescent strategy for liver capillary labeling with carbon quantum dot-lectin nanoprobe. Analyst, The, 2022, 147, 1952-1960.	1.7	3
158	Vibrational spectroscopic encoding of polystyrene-based resin beads: Converting the encoding peaks into barcodes. Spectrochimica Acta - Part A: Molecular and Biomolecular Spectroscopy, 2005, 62, 1039-1044.	2.0	2
159	Fluorescence Characteristics of CdTe Quantum Dot Colloids below the Freezing Point. Journal of Physical Chemistry C, 2021, 125, 9916-9922.	1.5	2
160	A nanoplatform of hollow Ag2S/Ag nanocomposite shell for photothermal and enhanced sonodynamic therapy mediated by photoacoustic and CT imaging. Chemical Engineering Journal, 2022, 433, 133196.	6.6	2
161	Quantum Dots: Tracking the Downâ€Regulation of Folate Receptorâ€Î± in Cancer Cells through Target Specific Delivery of Quantum Dots Coupled with Antisense Oligonucleotide and Targeted Peptide (Small 24/2013). Small, 2013, 9, 4182-4182.	5.2	1
162	PEC-phospholipid-encapsulated bismuth sulfide and CdSe/ZnS quantum dot core–shell nanoparticle and its computed tomography/fluorescence performance. Journal of Nanoparticle Research, 2015, 17, 1.	0.8	1

#	Article	IF	CITATIONS
163	CdTe@CdS quantum dots for labeling and imaging macrophages in liver frozen sections below the freezing point. Journal of Materials Chemistry B, 2022, 10, 2952-2962.	2.9	1
164	Tumor Margin Demarcation and Therapy: A NanoFlareâ€Based Strategy for In Situ Tumor Margin Demarcation and Neoadjuvant Gene/Photothermal Therapy (Small 50/2018). Small, 2018, 14, 1870245.	5.2	0
165	Investigation of the bioactivity and fluorescence imaging of multicellular tumor spheroid targeted labelling with CdSe/ZnS quantum dots. Journal of Nanoparticle Research, 2022, 24, 1.	0.8	0